

5-15-2020

## Polystyrene-block-Polydimethylsiloxane as a Potential Silica Substitute for Polysiloxane Reinforcement

Liyang Shen

*Iowa State University*, lshen@iastate.edu

Tung-Ping Wang

*Iowa State University*, wangtp@iastate.edu

Fang-Yi Lin

*Iowa State University*

*See next page for additional authors*

Follow this and additional works at: [https://lib.dr.iastate.edu/cbe\\_pubs](https://lib.dr.iastate.edu/cbe_pubs)

 Part of the [Polymer Science Commons](#)

The complete bibliographic information for this item can be found at [https://lib.dr.iastate.edu/cbe\\_pubs/430](https://lib.dr.iastate.edu/cbe_pubs/430). For information on how to cite this item, please visit <http://lib.dr.iastate.edu/howtocite.html>.

---

# Polystyrene-block-Polydimethylsiloxane as a Potential Silica Substitute for Polysiloxane Reinforcement

## Abstract

Here we report microphase-separated poly(styrene-*block*-dimethylsiloxane) (PS-*b*-PDMS) as a reinforcing filler in PDMS thermosets that overcomes the long-standing problem of aging in the processing of silica-reinforced silicone. Surprisingly, PS-*b*-PDMS reinforced composites display comparable mechanical performance to silica-modified analogs, even though the modulus of PS is much smaller than that of silica and there is no evidence of percolation with respect to the rigid PS domains. We have found that a few unique characteristics contribute to the reinforcing performance of PS-*b*-PDMS. The strong self-assembly behavior promotes batch-to-batch repeatability by having well-dispersed fillers. The structure and size of the fillers depend on the loading and characteristics of both filler and matrix, along with the shear effect. The reinforcing effect of PS-*b*-PDMS is mostly brought by the entanglements between the corona layer of the filler and the matrix, rather than the hydrodynamic reinforcement of the PS phase.

## Disciplines

Chemical Engineering | Polymer Science

## Comments

This document is the Accepted Manuscript version of a Published Work that appeared in final form in *ACS Macro Letters*. To access the final edited and published work see DOI: [10.1021/acsmacrolett.0c00211](https://doi.org/10.1021/acsmacrolett.0c00211).

## Authors

Liyang Shen, Tung-Ping Wang, Fang-Yi Lin, Sabrina Torres, Thomas Robison, Sri Harsha Kalluru, Nacú B. Hernández, and Eric W. Cochran

# Polystyrene-*block*-Polydimethylsiloxane as a Potential Silica Substitute for Polysiloxane Reinforcement

Liyang Shen, Tung-ping Wang, Fang-Yi Lin, Sabrina Torres, Thomas Robison, Sri Harsha Kalluru, Nacú B. Hernández, and Eric W. Cochran\*



Cite This: *ACS Macro Lett.* 2020, 9, 781–787



Read Online

ACCESS |



Metrics & More

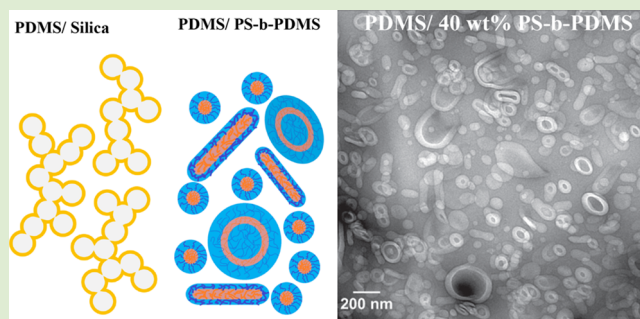


Article Recommendations



Supporting Information

**ABSTRACT:** Here we report microphase-separated poly(styrene-*block*-dimethylsiloxane) (PS-*b*-PDMS) as a reinforcing filler in PDMS thermosets that overcomes the long-standing problem of aging in the processing of silica-reinforced silicone. Surprisingly, PS-*b*-PDMS reinforced composites display comparable mechanical performance to silica-modified analogs, even though the modulus of PS is much smaller than that of silica and there is no evidence of percolation with respect to the rigid PS domains. We have found that a few unique characteristics contribute to the reinforcing performance of PS-*b*-PDMS. The strong self-assembly behavior promotes batch-to-batch repeatability by having well-dispersed fillers. The structure and size of the fillers depend on the loading and characteristics of both filler and matrix, along with the shear effect. The reinforcing effect of PS-*b*-PDMS is mostly brought by the entanglements between the corona layer of the filler and the matrix, rather than the hydrodynamic reinforcement of the PS phase.



Polydimethylsiloxane elastomer, commonly known as silicone rubber, has outstanding performance in a wide temperature range and is widely used in aviation and aerospace applications.<sup>1,2</sup> However, unfilled silicone rubbers, such as polydimethylsiloxane (PDMS), have poor mechanical properties because of the flexible polymer chain, thus, making reinforcement by filler essential. It is well-known that reinforcement by fillers improves the mechanical properties dramatically, which involves a hydrodynamic effect brought by the inclusion of rigid particles, matrix–filler, and filler–filler interactions.<sup>3,4</sup> Silica is widely used for silicone rubber reinforcement because of the high modulus and strong matrix–filler bonding.<sup>5–7</sup> Unfortunately, silica-filled silicone compounds require a few weeks’ storage, called “bin-aging”, for optimal physical properties before subsequent processing and vulcanization.<sup>2,8,9</sup> The precured compounds (silicone crepe) exhibit aging phenomena over long-term storage time,<sup>4</sup> including both hardening<sup>2,4–11</sup> and softening.<sup>12,13</sup> The inhibiting methods include adding plasticizers<sup>14</sup> and pretreatment of the silica surface.<sup>4</sup> However, remilling is usually required before further processing, which pushes up the cost and, more importantly, decreases the process repeatability.

Other than using inorganic fillers, it is also possible to obtain reinforcement by introducing glassy polymer domains within the elastomer. Polymer blending is widely used in polymer modification because of easy processability.<sup>15</sup> PDMS/polystyrene (PS) blends that were prepared by in situ radical copolymerization of styrene in a PDMS matrix showed

improved mechanical properties, including 9-fold increased tensile strength at 43% PS loading in comparison with neat PDMS elastomer.<sup>16</sup> However, the mechanical properties of immiscible homopolymer blends are still poor because of the lack of adhesion among the constituent components, which originates from strong repulsive thermodynamic interactions.<sup>17</sup> Block copolymers formed from two or more polymer blocks with distinct properties may be another solution. The microscopic segregation of these blocks can generate complex structures and desirable properties. Block copolymers are widely applied as the well-known thermoplastic elastomers, which are composed of hard and soft polymer blocks.<sup>18</sup> The outstanding strength and toughness are brought by the deformable plastic microdomains from microscopic phase separation. The PDMS–PS multiblock copolymers showed effective mechanical reinforcement with 30–50 wt % polystyrene.<sup>19</sup>

For the PDMS with various thermoplastics, vulcanization is unnecessary and the elastomers result from directly cooling the melt.<sup>4</sup> However, the extensibility is impaired without cross-

**Received:** March 13, 2020

**Accepted:** May 12, 2020



linking. A cross-linked block copolymer-filled PDMS composite may therefore be a preferential strategy to optimize the strength and extensibility. Several works in glassy polymer toughening have shown that block copolymers are able to act effectively at low concentration in blends with homopolymers. For example, epoxies can be toughened with trivial processing by using block copolymer self-assembly at low (5 wt %) block copolymer concentrations.<sup>20–22</sup> Low molar mass poly-(butylene oxide)-containing diblock copolymers at 5–10 wt % loading can be used as modifiers to toughen poly(lactide).<sup>23</sup>

Inspired by this strategy, we hypothesized that filler–matrix interactions in a block copolymer-reinforced PDMS thermoset could contribute to reinforcement more than hydrodynamic effects, which depend on the modulus and volume fraction of filler. Therefore, the favorable interactions between the PDMS block of a simple diblock copolymer and the PDMS matrix can enhance mechanical reinforcement. The self-assembly behavior of block copolymers is also a unique advantage over silica, which leads to microscopic phase separation and improves filler dispersion. PS is a well-studied choice as a reinforcing hard segment that can be easily synthesized with well-controlled polymerization. PS–PDMS materials were thus evaluated as fillers in PDMS having much better miscibility than homopolystyrene.<sup>24,25</sup> As demonstrated below, the comparison between the reinforcing effects of PDMS-*b*-PS and silica reveals the potential of the block copolymer to be a silica substitute.

The molecular characteristics of the two main polymeric materials are included in Table 1. To control the molecular

**Table 1. Molecular Characteristics of PDMS Homopolymer Matrix and PS-*b*-PDMS Diblock Copolymer<sup>a</sup>**

sample	$M_n$ (kg/mol)	$M_w/M_n$	$f_{PS\%}$	$w_{PS\%}$
vinyl-terminated PDMS	28	1.57		
diBCP	61	1.08	0.47	0.49

<sup>a</sup>diBCP represents PDMS-*b*-PS diblock copolymer. Number-average molecular weight and dispersity were determined by gel permeation chromatography. Volume and weight fraction calculated based on <sup>1</sup>H NMR results by using densities  $\rho_{PDMS} = 0.97$  g/cm<sup>3</sup><sup>26</sup> and  $\rho_{PS} = 1.05$  g/cm<sup>3</sup>.<sup>27</sup>

weight precisely, anionic polymerization was adopted to synthesize volume symmetric PS-*b*-PDMS (diBCP) with narrow molecular weight distribution.<sup>28–31</sup> The synthetic methods and molecular characterization are available in the Supporting Information. Vinyl-terminated polydimethylsiloxane (Gelest, DMS-V31 28 kDa) was used as the polymer matrix. The molecular weight of each block was chosen close to that of the PDMS matrix. The molecular weights of PDMS matrix and PDMS block of diBCP are around the critical value of linear PDMS chain entanglement, which is approximately 30 kg/mol.<sup>32</sup>

Spherical micelles, wormlike or cylindrical micelles, and closed “bags” formed by flat bilayers called vesicles under certain circumstances are the three basic structures from self-assembly when diblock copolymers dissolve in selective solvents or mix with polymer matrices.<sup>33</sup> In this work, the PDMS matrix acts as the good “solvent” for the PDMS block and a nonsolvent for the PS block. Figures 1 and S7 show representative transmission electron microscopy (TEM) images of all diBCP/PDMS blends at low and high magnification, respectively. The experimental methods of

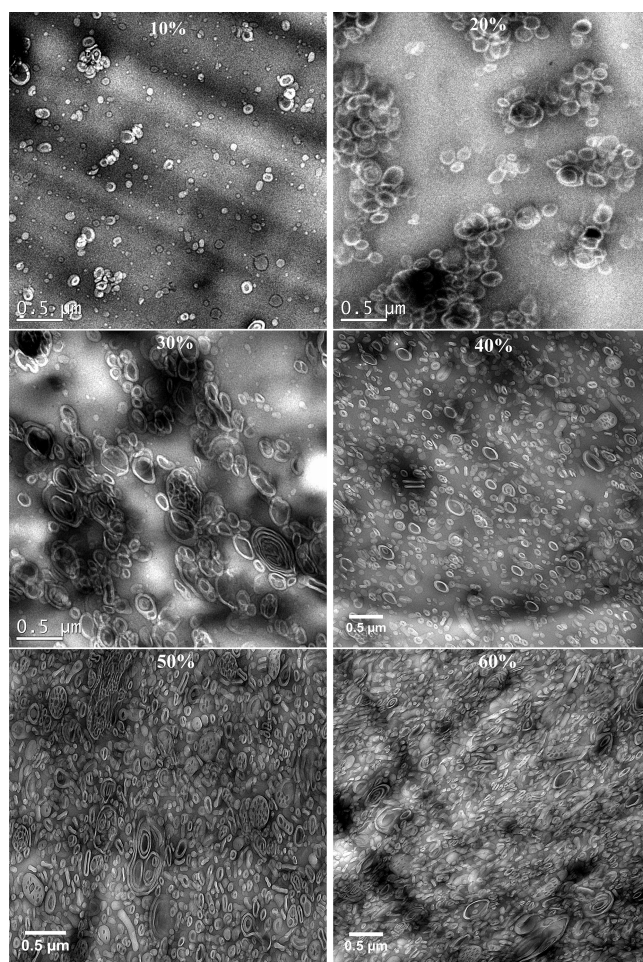


**Figure 1.** Representative TEM images of cryo-ultramicrotomed PDMS composites with PS-*b*-PDMS loading from 10 wt % to 60 wt %. Scale bars are all 0.5  $\mu$ m.

sample preparation and morphological characterization are included in the Supporting Information. Though the results of thermal characterization, which are shown in Figure S6, suggest complete incompatibility between PS and PDMS phases by no shift of the glass transition temperature of PS, the fillers are well-dispersed, and no macrophase separation is observed. As expected, the diBCP forms micelles and vesicles with different sizes and structures in the polymer matrix. It indicates that 10 wt % is above critical micelle concentration (CMC), and the compounding temperature is above the critical micelle temperature.

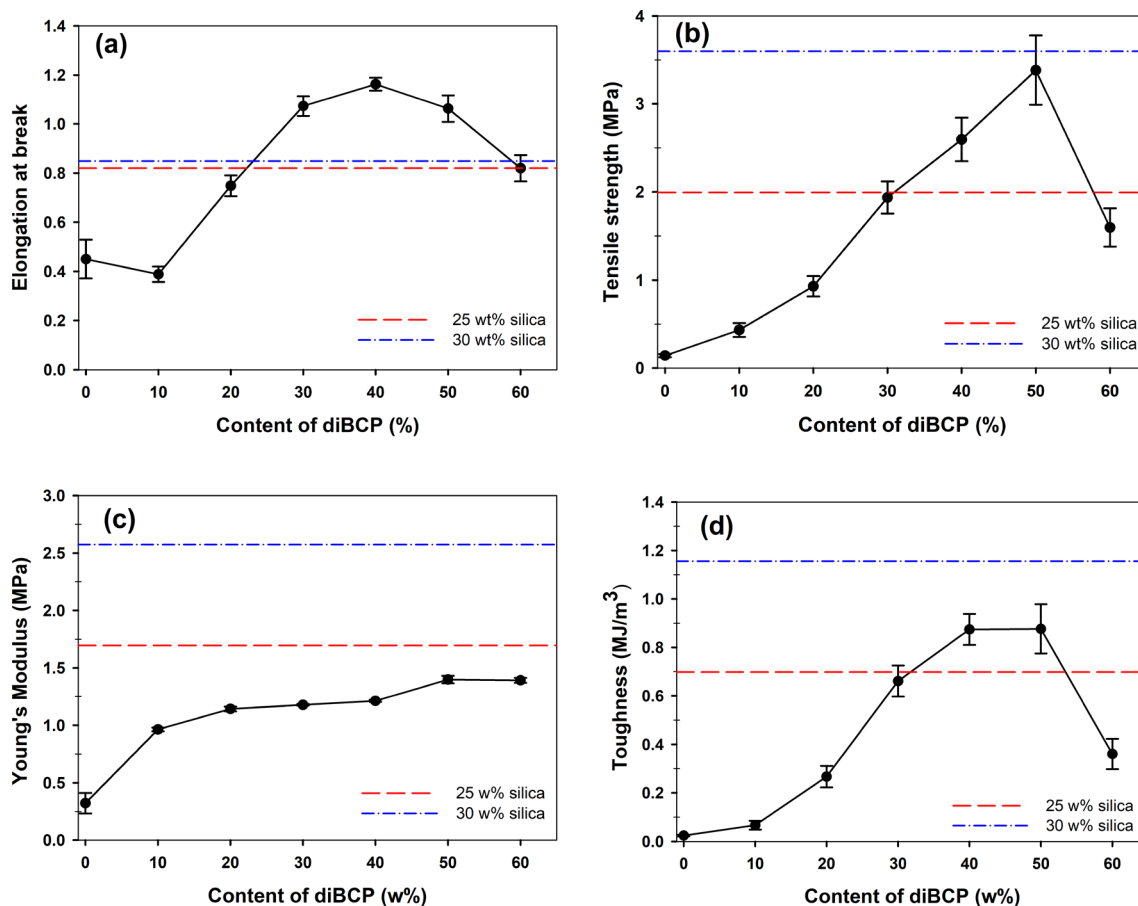
Several parameters, such as diBCP concentration and the molecular weights of both diBCP and homopolymer matrix, affect the structure of self-assembled diBCP.<sup>34</sup> A homogeneous phase occurs in which the diBCP is molecularly dispersed as solute in the homopolymer matrix if diBCP concentration is below the CMC. Within a certain concentration range above the CMC, independent micelles are dispersed in the homopolymer without long-range ordering. The sample with 10% diBCP loading reveals such morphology; as the diBCP concentration is increased further, fillers begin to contact, aggregate, and overlap, shown by the morphology of samples with 20–60 wt % diBCP loading. Under current blending conditions, the low-diBCP loading blends (below 50%) may reach the thermodynamic equilibrium based on the size distribution of the micelles. Further increasing the diBCP



**Table 2. Structural Parameters Extracted from SAXS Analysis of PDMS-*b*-PS Filled PDMS Samples Using the Core-Shell Model<sup>a</sup>**

sample	core radius ( $R_c$ , nm)	relative core polydispersity ( $\sigma/R_c$ )	shell thickness ( $T_s$ , nm)	scattering length density (SLD, $\times 10^{-6} \text{ \AA}^{-2}$ )		
				core ( $\rho_c$ )	shell ( $\rho_s$ )	matrix ( $\rho_0$ )
10 wt % diBCP	$9.30 \pm 0.43$	$0.78 \pm 0.05$	$51.9 \pm 0.38$	9.9	8.9	8.9
20 wt % diBCP	$42.5 \pm 0.40$	$0.53 \pm 0.01$	$15.3 \pm 0.10$	9.0	10.1	9.2

<sup>a</sup>Theoretical SLD:<sup>44</sup> PDMS ( $(\text{C}_2\text{H}_6\text{OSi})_n$ , 0.97 g/cm<sup>3</sup>) SLD:  $9.0 \times 10^{-6} \text{ \AA}^{-2}$  (Cu K $\alpha$ ); PS ( $(\text{C}_8\text{H}_8)_n$ , 1.05 g/cm<sup>3</sup>) SLD:  $9.6 \times 10^{-6} \text{ \AA}^{-2}$  (Cu K $\alpha$ ).

**Figure 2.** Effect of PS-*b*-PDMS content on mechanical properties of PDMS composites and the comparison with 25 and 30 wt % silica-filled PDMS composites: (a) Elongation at break; (b) Tensile strength; (c) Young's modulus; and (d) Toughness

concentration will typically induce a transition from spherical to cylindrical micelles,<sup>35</sup> as well as larger vesicles and multilamellar vesicles with “onion-like structures”.<sup>20</sup> However, the morphology of samples with 20–40 wt % diBCP loading shows that most of the vesicles remain unilamellar and even shrink instead of becoming larger and multilamellar. If the diBCP concentration keeps increasing, a transition to well-ordered periodic phases, such as lamellae and cylinders, should take place, where the homopolymers act to swell its corresponding domain of the diBCP.<sup>34</sup> However, no ordered structures are observed from the morphology of samples with 50 and 60 wt % diBCP loading. The intense shear flow brought by twin-screw compounding is the unique effect on those unusual behaviors. A small-angle X-ray scattering (SAXS) comparison of the samples with and without shearing is shown in Figure S10; evidently, shearing inhibits the formation of ordered structures and introduces kinetically trapped morphologies. It has been reported that smaller unilamellar vesicles or with less shells are formed with increasing shear rate in an

aqueous system,<sup>36</sup> and cylindrical micelles or bilayer tubes are also developed from the deformation of elongated vesicles under strong shearing.<sup>37</sup> More cylindrical micelles are observed from the morphologies of samples with 40 wt % to 60 wt % diBCP loading than that of samples with low diBCP loading. The formation of larger and multilamellar vesicles are restrained by the high shear flow, which leads to structures with a smaller curvature, such as cylindrical micelles and lamellar phases.<sup>38</sup> The shear-induced morphology is then trapped by the high temperature curing process. Similar behavior has been observed in a block copolymer melt, the phases formed after the shear-induced network-to-network transition are stable to annealing for a long time.<sup>39</sup> It indicates that shearing process can be a suitable method for morphology control in block copolymer/homopolymer blends.

The volume fraction of each block in the diBCP will also affect the structure of self-assembled diBCP. If the length of the insoluble block is larger than that of the soluble block in the preferential solvent, it tends to form vesicles. Conversely,

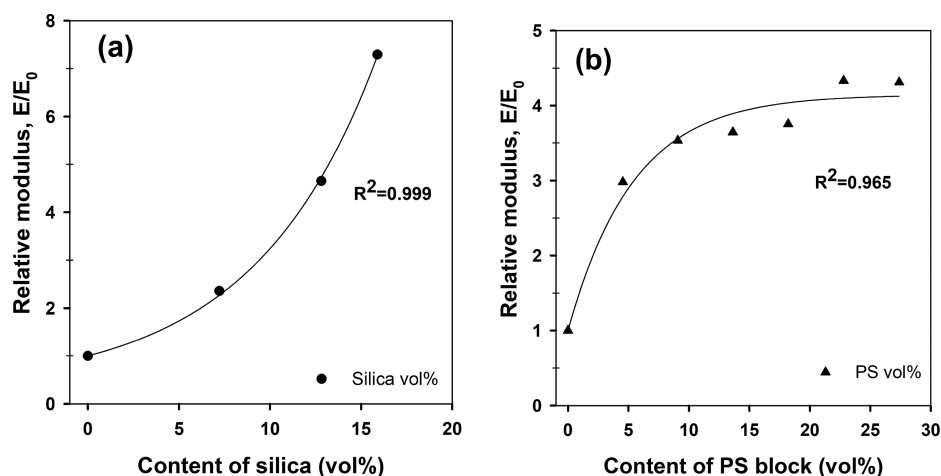


**Figure 3.** Relative Young's modulus  $E/E_0$  as a function of filler volume fraction and model fitting: (a) silica (circles) and (b) PS block of PS-*b*-PDMS (triangles).  $E_0 = 0.32$  MPa.

spherical micelles will be formed.<sup>21,40,41</sup> This effect is controlled since the two blocks are approximately symmetric. The disparity between molecular weights of diBCP and homopolymer matrix can affect the dimensions of self-assembled diBCP. In the case of diBCP spherical micelles, if the molecular weight of the soluble block of diBCP is similar or higher than the homopolymer matrix, the corona can be swelled by the homopolymer matrix and has larger thickness.<sup>34</sup> On the contrary, the corona cannot be swollen if the molecular weight of soluble block of diBCP is much lower than that of matrix. The micelles with swelled corona have stronger filler–matrix interactions and, therefore, are more stable, because the free homopolymer chains penetrate the soluble block chains and force them to extend into the matrix.<sup>42</sup>

SAXS profiles with form factor fits of 10 and 20 wt % diBCP loaded samples at room temperature are shown in Figure S8. For the samples with higher loading, the diversity of particle size and shape interferes with the form factor fitting intensely, as well as strong interparticle correlations due to the dense particle concentration revealed by TEM images. The structures studied here are spherical micelles and vesicles according to theoretical prediction and TEM images. The fitting is based on a core–shell model, which can fit the transitional structures more universally than models based on single structure, such as polymer micelle model;<sup>43</sup> the details are included in the Supporting Information.

Table 2 shows the quantitative information on size and distribution from the SAXS models. For spherical micelles, the core consists of PS microdomains and the shell can be ascribed to the PDMS phase swelled by PDMS matrix. For vesicles, PS formed the shell and the core is the PDMS block of the diBCP. The data are described by this model very well as can be seen from the fitting results. The 10 wt % diBCP loaded sample has a smaller core size and larger shell thickness since the densely packed PS block formed the core and the chains of PDMS block are unperturbed in PDMS matrix. The 20 wt % diBCP loaded sample has a relatively smaller PDMS domain size due to the constraint of PS shell. The bilayer walls of vesicle have approximately doubled PS domain size. The values of polydispersity indicate that these samples formed micelles in broad size distribution, which are confirmed by TEM images.

The stress–strain curves of neat PDMS, 10–60 wt % diBCP-loaded PDMS composites are shown in Figure S5,

which are compared with that of silica-filled composites. The details of sample preparation and tensile tests are included in the Supporting Information. The associated tensile strength, Young's modulus, elongation at break, and toughness are summarized in Table S1. The effect of diBCP content on the four mechanical properties is illustrated in Figure 2. Overall, the diBCP addition enhances all four mechanical properties dramatically compared to the neat PDMS. The high degree of sample-to-sample reproducibility indicates evenly dispersed fillers and microscopic phase separation.

The mechanical properties have increasing values with higher diBCP loading, and the overall optimal condition is at 50 wt % loading. The result indicates that increasing PS content does improve strength as expected. All BCP-filled samples have similar linear behavior at small strain, suggesting that the deformation of samples remains Hookean. The 50 and 60 wt % loading samples have an abrupt increase in modulus at large strain. Natural rubber has a similar behavior due to strain-induced crystallization.<sup>45</sup> However, the PDMS matrix is rubbery at room temperature, since  $T_g$  and  $T_c$  are well below 20 °C.<sup>4</sup> The stress increase is more likely caused by limited extensibility of the network according to the non-Gaussian statistical theory.<sup>46</sup> The effect of diBCP content on toughness is similar to tensile strength and elongation at break since larger value of stress and strain at break increases the energy absorption during extension.

Figure 3 shows the relative Young's modulus of silica and diBCP filled samples as a function of filler volume fraction. The data of PDMS/silica samples are fit by the model containing the well-known Guth and Gold equation<sup>47</sup> that accounts for the hydrodynamic effect and an additional exponential term with two adjustable coefficients to accommodate the conspicuous increase at high filler loading due to the rearrangement of filler at high loading,<sup>48</sup> which is eq 1:

$$\frac{E}{E_0} = 1 + 2.5\phi + 14.1\phi^2 + A(e^{B\phi} - 1)$$

$$A = 0.462, \quad B = 16.10 \quad (1)$$

Unlike the exponential growth behavior of PDMS/silica samples, the diBCP-filled samples exhibit a possible upper limit. The empirical equation is therefore modified with an exponential decay term in increasing form with two adjustable

coefficients and has the Guth–Gold equation removed, which is eq 2:

$$\frac{E}{E_0} = 1 + A(1 - e^{-B\phi})$$
$$A = 3.145, B = 18.50 \quad (2)$$

The reinforcing effect brought by silica can be contributed by the hydrodynamic effect of rigid particle inclusion, the filler–matrix interactions on the silica surface, and filler–filler interaction. For the diBCP-filled PDMS, to correlate the mechanical properties with morphology, the increasing interfacial area of self-assembled diBCP could contribute to the improvement of mechanical properties with increasing diBCP loading. Unlike the aggregates and percolation network of the silica fillers, the PS micelle cores are unable to contact each other directly to form the percolation network. The interfacial adhesive force between the PS and PDMS phases is brought by the physical entanglements of PDMS chains and the covalent bonding between PS and PDMS phases within diBCP. The reinforcing effect brought by the filler–matrix interaction is weak at low-diBCP loading because of small interfacial area. With higher loading of diBCP, the increasing number of micelles, vesicles and their aggregations enlarge the interface area between filler and matrix, and therefore enhance the mechanical properties. As the interfacial area increases rapidly with the content of diBCP at the early stage and then reaches to a limit, so does the modulus, which can be fit by the exponential decay term. However, the sample with 60 wt % loading becomes weaker. The breakage at smaller strain suggests the cross-linking network became less stable, which may be caused by overlapping and stacking of fillers. The interaction energy of two overlapping micelles is repulsive and the concentration of homopolymer chains in the outer shell decreases, which impairs the entanglement.<sup>49</sup> On the other hand, the sample with 60 wt % loading has only 40 wt % vinyl-terminated PDMS matrix, which is the component that takes part in cross-linking, shown in Scheme S2. The PDMS block of diBCP does not react with the cross-linking agents during the platinum-catalyzed reaction. When the block copolymer filler content is over 50%, the modulus is affected by the decrease of the cross-linkable PDMS matrix content.

The comparison with the mechanical properties of silica-reinforced samples shows the great potential of the polystyrene-based block copolymers as reinforcing fillers, even with respect to commercially available silica reinforced PDMS composites.<sup>50</sup> The performance of 50 wt % diBCP loaded sample is taken as example. The tensile strength rivals that of 30 wt % silica loaded sample and out-performs 25 wt % silica, while boasting larger elongation-at-break. For Young's modulus, the value is about 80% of that of 25 wt % silica and 50% of that of 30 wt % silica, which is remarkable since the modulus of homopolystyrene is less than one tenth of that of silica.<sup>51</sup>

In conclusion, a proof-of-concept strategy to substitute silica by PS-*b*-PDMS as reinforcing filler for PDMS composites has been successfully proposed and verified experimentally. The glassy PS phase as part of PS-*b*-PDMS diblock copolymer has shown prominent reinforcing effect on PDMS. The PDMS composites with 50 wt % loading have the optimal mechanical properties, such as tensile strength. The comparison with the silica filled samples shows the potential of this polymer filler. Although the modulus of PS is much smaller than silica, the

PS-*b*-PDMS filled composites exhibit similar mechanical performance as silica filled composites. The well-defined diblock copolymer is essential to provide controlled self-assembly structures, which brings better filler dispersion and promotes filler–matrix interactions. The increased interfacial area and adhesive force also enhance the mechanical properties. In addition, the shear effect during blending is a suitable method for morphology control in block copolymer/homopolymer blends.

## ■ ASSOCIATED CONTENT

### Supporting Information

The Supporting Information is available free of charge at <https://pubs.acs.org/doi/10.1021/acsmacrolett.0c00211>.

Experimental details and additional data (Schemes S1 and S2, Figures S1–S10, and Tables S1–S3) (PDF)

## ■ AUTHOR INFORMATION

### Corresponding Author

Eric W. Cochran – Department of Chemical and Biological Engineering, Iowa State University, Ames, Iowa 50011, United States; [orcid.org/0000-0003-3931-9169](https://orcid.org/0000-0003-3931-9169); Email: [ecochran@iastate.edu](mailto:ecochran@iastate.edu)

### Authors

Liyang Shen – Department of Chemical and Biological Engineering, Iowa State University, Ames, Iowa 50011, United States; [orcid.org/0000-0001-9928-2877](https://orcid.org/0000-0001-9928-2877)

Tung-ping Wang – Department of Chemical and Biological Engineering, Iowa State University, Ames, Iowa 50011, United States; [orcid.org/0000-0001-6292-3933](https://orcid.org/0000-0001-6292-3933)

Fang-Yi Lin – Department of Chemical and Biological Engineering, Iowa State University, Ames, Iowa 50011, United States; [orcid.org/0000-0002-7235-2596](https://orcid.org/0000-0002-7235-2596)

Sabrina Torres – Kansas City National Security Campus, Kansas City, Missouri 64147, United States

Thomas Robison – Kansas City National Security Campus, Kansas City, Missouri 64147, United States

Sri Harsha Kalluru – Department of Chemical and Biological Engineering, Iowa State University, Ames, Iowa 50011, United States; [orcid.org/0000-0003-2001-2896](https://orcid.org/0000-0003-2001-2896)

Nacú B. Hernández – Department of Chemical and Biological Engineering, Iowa State University, Ames, Iowa 50011, United States

Complete contact information is available at:

<https://pubs.acs.org/10.1021/acsmacrolett.0c00211>

### Notes

The authors declare no competing financial interest.

## ■ ACKNOWLEDGMENTS

The authors gratefully acknowledge the financial support of Honeywell Federal Manufacturing and Technology through Contract Nos. N000217245 and N000254419, administered by Dr. Sabrina Torres. This work benefited from the National Science Foundation, DMR-1626315, and the use of SasView application, originally developed under NSF Award No. DMR-0520547. SasView contains code developed with funding from the European Union's Horizon 2020 research and innovation programme under the SINE2020 Project, Grant Agreement No. 654000.



## REFERENCES

- (1) Blow, C. M. The Development and Testing of Elastomeric Materials for Fluid Sealing Applications. *Aircr. Eng.* **1964**, *36*, 208–212.
- (2) Southwart, D. W. Silicone rubbers: effect of silica fillers on processibility and properties. *Thesis*, Loughborough University, 1974.
- (3) Boonstra, B. B. Role of particulate fillers in elastomer reinforcement: a review. *Polymer* **1979**, *20*, 691–704.
- (4) Warrick, E. L.; Pierce, O. R.; Polmanteer, K. E.; Saam, J. C. Silicone elastomer developments 1967–1977. *Rubber Chem. Technol.* **1979**, *52*, 437–525.
- (5) Huang, X.; Fang, X.; Lu, Z.; Chen, S. Reinforcement of polysiloxane with superhydrophobic nanosilica. *J. Mater. Sci.* **2009**, *44*, 4522–4530.
- (6) Jia, L.; Du, Z.; Zhang, C.; Li, C.; Li, H. Reinforcement of polydimethylsiloxane through formation of inorganic-organic hybrid network. *Polym. Eng. Sci.* **2008**, *48*, 74–79.
- (7) Konkole, G. M.; McHard, J. A.; Polmanteer, K. E. Siloxane elastomers compounded with hydroxylated silanes. U.S. Patent 2,890,188, 1959.
- (8) Frank, F. Silicone compounds and elastomers prepared therefrom. U.S. Patent 2,954,357, 1960.
- (9) Hawley, M. E.; Wroblewski, D. A.; Orler, E. B.; Houlton, R.; Chitanvis, K. E.; Brown, G. W.; Hanson, D. E. Mechanical properties and filler distribution as a function of filler content in silica filled pdms samples. *MRS Online Proc. Libr.* **2003**, *791*, na.
- (10) Akoum, R. A.; Vault, C.; Schwartz, D.; Hirn, M.; Haidar, B. How silanization of silica particles affects the adsorption of PDMS chains on its surface. *J. Polym. Sci., Part B: Polym. Phys.* **2010**, *48*, 2371–2378.
- (11) Vondráček, P.; Schätz, M. Bound rubber and “crepe hardening” in silicone rubber. *J. Appl. Polym. Sci.* **1977**, *21*, 3211–3222.
- (12) DeGroot, J., Jr; Macosko, C. Aging phenomena in silica-filled polydimethylsiloxane. *J. Colloid Interface Sci.* **1999**, *217*, 86–93.
- (13) Selimovic, S.; Maynard, S. M.; Hu, Y. Aging effects of precipitated silica in poly (dimethylsiloxane). *J. Rheol.* **2007**, *51*, 325–340.
- (14) Schnurrbusch, K.; Kniege, W. Structure control additive for convertible organopolysiloxanes, and preparation thereof. U.S. Patent 3,551,382, 1970.
- (15) Utracki, L. A.; Wilkie, C. A. *Polymer Blends Handbook*; Springer, 2002; Vol. 1.
- (16) Fu, F. S.; Mark, J. E. Elastomer reinforcement from a glassy polymer polymerized in situ. *J. Polym. Sci., Part B: Polym. Phys.* **1988**, *26*, 2229–2235.
- (17) Utracki, L. A. Compatibilization of polymer blends. *Can. J. Chem. Eng.* **2002**, *80*, 1008–1016.
- (18) Bates, F. S.; Fredrickson, G. Block copolymers-designer soft materials. *Phys. Today* **1999**, *52*, 32.
- (19) Saam, J. C.; Fearon, F. G. Properties of polystyrene-polydimethylsiloxane block copolymers. *Ind. Eng. Chem. Prod. Res. Dev.* **1971**, *10*, 10–14.
- (20) Dean, J. M.; Lipic, P. M.; Grubbs, R. B.; Cook, R. F.; Bates, F. S. Micellar structure and mechanical properties of block copolymer-modified epoxies. *J. Polym. Sci., Part B: Polym. Phys.* **2001**, *39*, 2996–3010.
- (21) Dean, J. M.; Grubbs, R. B.; Saad, W.; Cook, R. F.; Bates, F. S. Mechanical properties of block copolymer vesicle and micelle modified epoxies. *J. Polym. Sci., Part B: Polym. Phys.* **2003**, *41*, 2444–2456.
- (22) Dean, J. M.; Verghese, N. E.; Pham, H. Q.; Bates, F. S. Nanostructure Toughened Epoxy Resins. *Macromolecules* **2004**, *37*, 1998–1998a.
- (23) Li, T.; Zhang, J.; Schneiderman, D. K.; Francis, L. F.; Bates, F. S. Toughening glassy poly (lactide) with block copolymer micelles. *ACS Macro Lett.* **2016**, *5*, 359–364.
- (24) Chuai, C. Z.; Li, S.; Almdal, K.; Alstrup, J.; Lyngaae-Jørgensen, J. The effect of compatibilization and rheological properties of polystyrene and poly (dimethylsiloxane) on phase structure of polystyrene/poly (dimethylsiloxane) blends. *J. Polym. Sci., Part B: Polym. Phys.* **2004**, *42*, 898–913.
- (25) Hu, W.; Koberstein, J. T.; Lingelser, J. P.; Gallot, Y. Interfacial tension reduction in polystyrene/poly (dimethylsiloxane) blends by the addition of poly (styrene-*b*-dimethylsiloxane). *Macromolecules* **1995**, *28*, 5209–5214.
- (26) Kataoka, T.; Ueda, S. Viscosity–molecular weight relationship for polydimethylsiloxane. *J. Polym. Sci., Part B: Polym. Lett.* **1966**, *4*, 317–322.
- (27) Fox, T. G., Jr; Flory, P. J. Second-order transition temperatures and related properties of polystyrene. I. Influence of molecular weight. *J. Appl. Phys.* **1950**, *21*, 581–591.
- (28) Bajaj, P.; Varshney, S. K.; Misra, A. Block copolymers of polystyrene and poly (dimethyl siloxane). I. Synthesis and characterization. *J. Polym. Sci., Polym. Chem. Ed.* **1980**, *18*, 295–309.
- (29) Chu, J. H.; Rangarajan, P.; Adams, J. L.; Register, R. A. Morphologies of strongly segregated polystyrene-poly (dimethylsiloxane) diblock copolymers. *Polymer* **1995**, *36*, 1569–1575.
- (30) Saam, J. C.; Gordon, D. J.; Lindsey, S. Block copolymers of polydimethylsiloxane and polystyrene. *Macromolecules* **1970**, *3*, 1–4.
- (31) Zilliox, J. G.; Roovers, J. E. L.; Bywater, S. Preparation and properties of polydimethylsiloxane and its block copolymers with styrene. *Macromolecules* **1975**, *8*, 573–578.
- (32) Bagley, E.; West, D. Chain Entanglement and Non-Newtonian Flow. *J. Appl. Phys.* **1958**, *29*, 1511–1512.
- (33) Hiemenz, P. C.; Lodge, T. P. *Polymer Chemistry*; CRC Press, 2007; pp 129–131.
- (34) Kinning, D. J.; Thomas, E. L.; Fetters, L. J. Morphological studies of micelle formation in block copolymer/homopolymer blends. *J. Chem. Phys.* **1989**, *90*, 5806–5825.
- (35) Kinning, D. J.; Winey, K. I.; Thomas, E. L. Structural transitions from spherical to nonspherical micelles in blends of poly (styrene-butadiene) diblock copolymer and polystyrene homopolymers. *Macromolecules* **1988**, *21*, 3502–3506.
- (36) Bergmeier, M.; Gradzielski, M.; Hoffmann, H.; Mortensen, K. Behavior of a charged vesicle system under the influence of a shear gradient: a microstructural study. *J. Phys. Chem. B* **1998**, *102*, 2837–2840.
- (37) Shahidzadeh, N.; Bonn, D.; Aguerre-Chariol, O.; Meunier, J. Large deformations of giant floppy vesicles in shear flow. *Phys. Rev. Lett.* **1998**, *81*, 4268.
- (38) Butler, P. Shear induced structures and transformations in complex fluids. *Curr. Opin. Colloid Interface Sci.* **1999**, *4*, 214–221.
- (39) Cochran, E. W.; Bates, F. S. Shear-induced network-to-network transition in a block copolymer melt. *Phys. Rev. Lett.* **2004**, *93*, 087802.
- (40) Blanazs, A.; Madsen, J.; Battaglia, G.; Ryan, A. J.; Armes, S. P. Mechanistic insights for block copolymer morphologies: how do worms form vesicles? *J. Am. Chem. Soc.* **2011**, *133*, 16581–16587.
- (41) Smart, T.; Lomas, H.; Massignani, M.; Flores-Merino, M. V.; Perez, L. R.; Battaglia, G. Block copolymer nanostructures. *Nano Today* **2008**, *3*, 38–46.
- (42) Borukhov, I.; Leibler, L. Stabilizing grafted colloids in a polymer melt: Favorable enthalpic interactions. *Phys. Rev. E: Stat. Phys., Plasmas, Fluids, Relat. Interdiscip. Top.* **2000**, *62*, R41.
- (43) Pedersen, J. S. Form factors of block copolymer micelles with spherical, ellipsoidal and cylindrical cores. *J. Appl. Crystallogr.* **2000**, *33*, 637–640.
- (44) Roe, R.-J. *Methods of X-ray and Neutron Scattering in Polymer Science*; Oxford Univ. Press, 2000; Vol. 739; pp 9–12.
- (45) Mark, J. E. The effect of strain-induced crystallization on the ultimate properties of an elastomeric polymer network. *Polym. Eng. Sci.* **1979**, *19*, 409–413.
- (46) Doherty, W. O. S.; Leè, K. L.; Treloar, L. R. G. Non-Gaussian effects in styrene-butadiene rubber. *Br. Polym. J.* **1980**, *12*, 19–23.
- (47) Guth, E. Theory of filler reinforcement. *J. Appl. Phys.* **1945**, *16*, 20–25.



(48) Thomas, D. G. Transport characteristics of suspension: VIII. A note on the viscosity of Newtonian suspensions of uniform spherical particles. *J. Colloid Sci.* **1965**, *20*, 267–277.

(49) Leibler, L.; Pincus, P. A. Ordering transition of copolymer micelles. *Macromolecules* **1984**, *17*, 2922–2924.

(50) Johnston, I.; McCluskey, D.; Tan, C.; Tracey, M. Mechanical characterization of bulk Sylgard 184 for microfluidics and micro-engineering. *J. Micromech. Microeng.* **2014**, *24*, 035017.

(51) Tao, R.; Simon, S. L. Bulk and shear rheology of silica/polystyrene nanocomposite: reinforcement and dynamics. *J. Polym. Sci., Part B: Polym. Phys.* **2015**, *53*, 621–632.